

Experimental Evaluation of Unberthing Manoeuvre Control Using an Online Estimation Model Under Actual Sea Conditions

H. Kashiwagi & T. Okazaki

Tokyo University of Marine Science and Technology, Tokyo, Japan

ABSTRACT: Ship manoeuvrability varies with speed and is affected by environmental disturbances, making unberthing control challenging. To address this, a control method using an online estimation model is proposed, in which the parameters of a linear motion model are sequentially updated based on the observed ship velocities and actuator inputs. A linear quadratic regulator was applied for route tracking, and a bias term was introduced to estimate and compensate for steady external forces, such as wind and tidal currents. The proposed method was validated through actual sea experiments using a full-scale vessel. The control system achieved accurate tracking using an unberthing manoeuvre. It also demonstrated effective disturbance compensation and adaptability to changes in actuator effectiveness. These results confirmed the practicality of the proposed approach for real-time unberthing operations under actual sea conditions.

1 INTRODUCTION

Recently, intensive research has been conducted on the development of automatic control technologies to bring maritime autonomous surface ships into practical service [1]. Among the various ship-handling tasks, berthing and unberthing manoeuvres in confined waters, such as ports, pose a significant challenge to automation because of the high control accuracy required. One contributing factor is the change in the manoeuvrability caused by acceleration and deceleration. The effectiveness of the rudder used for the heading control depends on the surrounding inflow velocity. Therefore, the controller must output commands that account for the variations in manoeuvrability caused by changes in speed and propeller thrust. Moreover, the influence of disturbances, such as wind and current, becomes relatively more significant when manoeuvrability is reduced. Consequently, in berthing and unberthing controls where speed changes are required, controllers

must be designed based on motion models that can represent such variations and disturbances.

Nonlinear motion models are often used to represent ship motions during berthing and unberthing, and several control methods based on such models have been proposed. Nonlinear models are capable of expressing speed-dependent nonlinear variations such as hull resistance and the effectiveness of actuators, thereby contributing to high control accuracy during acceleration and deceleration. The parameters of these nonlinear models have been identified through captive model tests in tanks, where scaled ship models were moved under constrained conditions [2]. However, tank experiments require large-scale facilities and extensive trials under various conditions, making them time-consuming and costly. As an alternative, methods have been proposed to estimate parameters from motion data acquired during free-running tests using model or full-scale ships [3–5]. These approaches enable the identification of motion

models from limited data, even for vessels with unknown motion characteristics. However, parameter estimation for nonlinear motion models generally requires high computational power and extended convergence times. The mathematical modelling group model [6] offers another approach in which empirical formulas derived from extensive experimental data across various ship types are used to estimate model parameters from principal particulars [7–9]. These formulas allow for the design of motion models without the need for physical experiments. Based on these formulas, Miyoshi et al. [10] designed a linear motion model, which was used for route-tracking and berthing control [11, 12]. This method was applied to three vessels and its effectiveness was demonstrated through experiments under actual sea conditions. Although linear models are relatively easy to design, they often require parameter tuning to accurately represent actual ship behaviour, leading to non-negligible implementation costs for each target ship. Furthermore, when controlling manoeuvres involving speed changes using linear models, an additional model design for various speed ranges is necessary [12]. To address these challenges, recent studies have proposed online model estimation methods that sequentially update the motion model parameters using input-output data acquired during manoeuvring [13]. These approaches allow for control without predefining a motion model by continuously updating it in real time. Nonetheless, for actual deployment in ship operations, linear models are preferred because of their predictability and reliability [11, 12].

To overcome this issue, the authors previously proposed a model estimation method that updates a linear model, initially derived from principal particulars, using input-output data obtained during control [14]. As the speed of a ship changes gradually, the associated changes in manoeuvrability are also gradual. Thus, sequential updates to linear model parameters can effectively capture speed-dependent variations in dynamics. The estimated parameters were those of the sway and yaw motions, which were controlled by the rudder in a three-degree-of-freedom linear model. In this model estimation, the time delay between the actuator inputs and the resulting motions was considered by shifting the input-output time series. In addition, to compensate for steady external disturbances, such as tidal currents, a bias term was introduced in the sway motion model to estimate the steady forces acting on the hull. The rudder command was then adjusted based on the estimated disturbance effect. The effectiveness of this method was previously verified using simulations of unberthing manoeuvres, showing that it can accurately reproduce ship motion even in the presence of sensor noise and current disturbances [14]. However, under actual sea conditions, multiple time-varying disturbances—such as wind and current—exist, and sensor data may contain irregular noise, which can affect both model estimation and control performance. Therefore, an experimental validation using an actual ship is necessary to demonstrate its practical effectiveness.

In this study, we implemented a control system based on the proposed online estimation model on a full-scale ship and evaluated its performance through real sea trials. The target ship was Shioji Maru, a 60 m long, 775-ton training ship comparable in size to a

typical 500-ton coastal cargo vessel. The control was conducted based on a manoeuvring plan created by referencing the actual unberthing operations of the target ship. The experiments were conducted in a large open-sea area within a bay to ensure the safety of the ship and surrounding structures, and virtual quays were defined to reproduce the unberthing scenario. Although the bank effects cannot be replicated, the setup allows for the evaluation of responses to wind and current disturbances. Owing to the operational limitations of the actuators, the unberthing manoeuvre is divided into two phases: unberthing and leaving. The implemented system included online model estimation and route-tracking control modules proposed in a previous study [14]. The model parameters were updated using the time-series data of the actuator inputs and the measured ship velocities via the gradient descent method. Based on the estimated linear model, a state-feedback controller using a linear quadratic regulator (LQR) algorithm is applied for route tracking. The model update and control frequency were set to 2 Hz in accordance with the system cycle of the ship. Moreover, the actuator commands from the control system were constrained according to the operational limits of the target ship to prevent overloading. The experimental results demonstrate that the proposed control method can estimate external disturbances and achieve accurate unberthing control under actual sea conditions.

The remainder of this paper is organized as follows. Section 2 describes the unberthing motion model used in this study. Section 3 presents the online model estimation method and control system. Section 4 describes the experimental setup and Section 5 presents the experimental results. Finally, Section 6 concludes the study.

2 SHIP MOTION MODEL IN UNBERTHING MANEUVER

2.1 *Manoeuvring Phases*

In this study, an unberthing manoeuvre is defined as an operation in which a ship departs from a stationary position on a quay and accelerates while following a planned course line. As shown in Figure 1, the unberthing manoeuvre is divided into two phases, the unberthing and leaving phases, based on the actuators used for attitude control. The unberthing phase refers to the initial stage of the manoeuvre when the ship away from the quay at speeds below 3 kn (5.6 km/h). In this phase, attitude control is achieved using side thrusters because rudder effectiveness is limited at low speeds. The leaving phase is defined as the stage at which the ship's speed exceeds 3 kn and continues to accelerate outward from the port. In this phase, control was performed using the main propeller and rudder, which become effective at higher speeds. Accordingly, different actuator configurations are used in the two phases. The unberthing phase employs the main propeller, bow thruster (B/T), and stern thruster (S/T), whereas the leaving phase uses the main propeller and rudder. In this study, separate motion models, parameter estimation processes, and controller designs were developed for each phase.

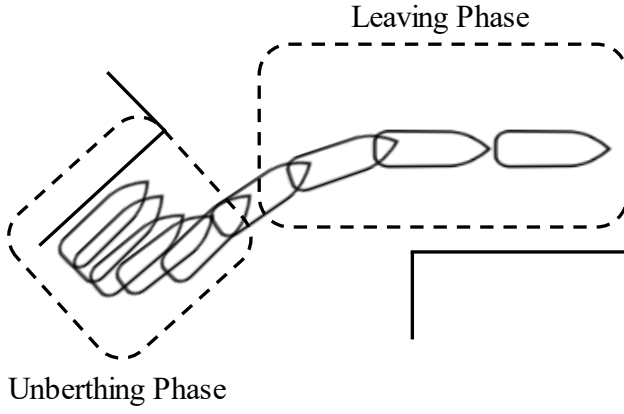


Figure 1. Manoeuvring phases in the unberthing manoeuvre

2.2 Ship motion model

In this study, a linear model was used to describe the motion of a ship to be able to apply the linear control theory. Because ship dynamics are inherently nonlinear, a steady-state condition is assumed, in which the ship is proceeding straight ahead at a constant speed U_s . The linear model represents variations in the state relative to the steady-state condition. The model describes the motion of a ship with three degrees of freedom—surge, sway, and yaw—using the coordinate system shown in Figure 2. Here, X and Y represent the longitudinal and lateral positions [m], respectively, ψ denotes the heading angle [rad], u denotes the surge speed [m/s], v denotes the sway speed [m/s], and r denotes the yaw rate [rad/s]. The actuator variables include the propeller blade angle θ_P [rad], the rudder angle δ [rad], B/T blade angle θ_B [rad], and the S/T blade angle θ_S [rad]. Positive values of these variables indicate the motion of the ship in the forward or starboard directions. The linear motion model with three degrees of freedom used in this study is express:

$$\dot{\mathbf{x}} = \mathbf{A}\mathbf{x} + \mathbf{B}\mathbf{u}$$

$$\mathbf{x} = [u \quad v \quad r]^T, \quad \mathbf{u} = [\theta_P \quad \delta \quad \theta_B \quad \theta_S]^T \quad (1)$$

$$\mathbf{A} = \begin{bmatrix} a_{uu} & 0 & 0 \\ 0 & a_{vv} & a_{vr} \\ 0 & a_{rv} & a_{rr} \end{bmatrix}, \quad \mathbf{B} = \begin{bmatrix} b_{uP} & 0 & 0 & 0 \\ 0 & b_{v\delta} & b_{vB} & b_{vS} \\ 0 & b_{r\delta} & b_{rB} & b_{rS} \end{bmatrix}$$

where \mathbf{x} is the state vector, and \mathbf{u} is the control input vector. \mathbf{A} is the system matrix a represents its elements, \mathbf{B} is the input matrix, and b represents its elements. Each of the element a and b uses subscripts, in which the first character indicates the left-hand-side state variable, and the second character indicates the state variable or control input to which the coefficient is applied. For example, a_{vr} refers to the coefficient multiplied by r in the equation for \dot{v} .

In this study, to enable discrete-time control with sampling period T_s [s], the continuous-time model in Equation (1) is discretized. The resulting discrete-time state-space model for the unberthing manoeuvre is expressed as follows:

$$\mathbf{x}(t+1) = \mathbf{\Phi}\mathbf{x}(t) + \mathbf{\Gamma}\mathbf{u}(t)$$

$$\mathbf{\Phi} = \begin{bmatrix} \varphi_{uu} & 0 & 0 \\ 0 & \varphi_{vv} & \varphi_{vr} \\ 0 & \varphi_{rv} & \varphi_{rr} \end{bmatrix}, \quad \mathbf{\Gamma} = \begin{bmatrix} \gamma_{uP} & 0 & 0 & 0 \\ 0 & \gamma_{v\delta} & \gamma_{vB} & \gamma_{vS} \\ 0 & \gamma_{r\delta} & \gamma_{rB} & \gamma_{rS} \end{bmatrix} \quad (2)$$

where $\mathbf{\Phi}$ is the state transition matrix and φ represents its elements; $\mathbf{\Gamma}$ is the input matrix and γ represents its elements. The subscript notation used for φ and γ follows the same rule as that for a and b in Equation (1). The matrices $\mathbf{\Phi}$ and $\mathbf{\Gamma}$ are derived as follows:

$$\mathbf{\Phi} = e^{\mathbf{A}T_s}$$

$$\mathbf{\Gamma} = \int_0^{T_s} e^{\mathbf{A}s} d\mathbf{s}\mathbf{B} \quad (3)$$

In this study, the control sampling period T_s is set to 0.5 s.

3 CONTROL SYSTEM USING AN ONLINE ESTIMATION MODEL

3.1 Control system overview

In this study, a control system was developed to perform an unberthing manoeuvre using an online estimation model. The system integrates model estimation and control functionalities into a unified application. It comprises four main components: model estimation, route-tracking controller design, disturbance compensation, and output command process. The computational flow of each control step is illustrated in Figure 3. Each system component is described in detail in the following section.

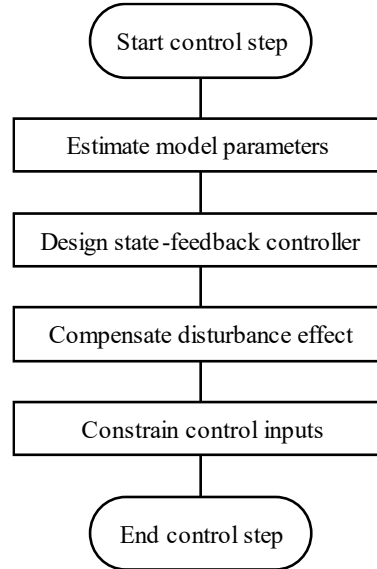


Figure 3. Flow diagram of the control system

3.2 Online model Estimation

The parameters of the linear model presented in Equation (2) were estimated online for the sway and yaw motions, which are controlled by the rudder, B/T, and S/T, and their effectiveness varies with the ship speed. The estimation was conducted using a batch gradient descent method, as in our previous study [14], based on the observed ship velocity and actuator input data. Because time delays between actuator inputs and

the resulting ship responses can affect the accuracy of the model estimation [15], the time-series input-output data were shifted according to the delay before being used in the parameter update process. Additionally, during unberthing, a ship is exposed to environmental disturbances such as tidal currents. These disturbances affect not only the route-tracking performance but also the model estimation accuracy because such effects are not included in the linear models [15]. To account for this, we introduced the bias term c_v into the sway motion model during the leaving phase, focusing on the steady component of environmental disturbances affecting sway. The models used to estimate the sway and yaw motions are given below. As the actuator configurations differ between the unberthing and leaving phases, Equation (4) is applied to the former, and Equation (5) to the latter:

$$\begin{aligned} v(n) &= \varphi_{vv}v(n-1) + \varphi_{vr}r(n-1) + \gamma_{v\delta}\delta(n-\tau_v) + \gamma_{vS}\theta_S(n-\tau_v) \\ r(n) &= \varphi_{rv}v(n-1) + \varphi_{rr}r(n-1) + \gamma_{rB}\theta_B(n-\tau_r) + \gamma_{rS}\theta_S(n-\tau_r) \end{aligned} \quad (4)$$

$$\begin{aligned} v(n) &= \varphi_{vv}v(n-1) + \varphi_{vr}r(n-1) + \gamma_{v\delta}\delta(n-\tau_v) + c_v \\ r(n) &= \varphi_{rv}v(n-1) + \varphi_{rr}r(n-1) + \gamma_{r\delta}\delta(n-\tau_r) \end{aligned} \quad (5)$$

Here, $v(n)$, $r(n)$, and $\delta(n)$ represent the sway speed, yaw rate, and rudder angle at time step n , respectively. The term c_v represents the bias force due to steady disturbance. The delays τ_v and τ_r denote the time delays [s] in the sway and yaw motions, respectively. Based on operational data from the target ship, τ_v and τ_r were set to 15 s and 10 s, respectively.

In the proposed estimation method, the parameters φ , γ , c_v and in Equations (4) and (5) are updated by minimizing the loss function L , which represents the squared error between the observed and predicted states. Loss function L is defined as follows:

$$L(n) = \frac{1}{T_r} \sum_{t=n-t_r}^n \{y(t) - \hat{y}(n)\}^2 \quad (6)$$

where T_r is the number of input-output data samples used in the estimation, y is the observed state (e.g., v or r), and \hat{y} is the predicted state from Equations (4) and (5). The model parameters are iteratively updated using the following gradient descent method:

$$\theta(n+1) = \theta(n) - \alpha \frac{\partial L}{\partial \theta} \quad (7)$$

where θ denotes the set of parameters to be estimated (e.g., φ , γ , and c_v), and α is the learning rate. In this study, the parameters were updated 100 times for each control cycle.

3.3 Route-tracking control

In this study, a state-feedback control approach was applied to enable a ship to follow a planned unberthing route based on the estimated linear model. The control design was obtained using an LQR algorithm, which minimizes the deviation from the planned route and the heading error between the ship's orientation and route direction, as illustrated in Figure 4., where X_d and Y_d represent the longitudinal and lateral distances [m] to the target waypoint, respectively; ψ_d denotes the heading error [rad] with respect to the desired

trajectory. The control model for the unberthing manoeuvres formulated separately for the unberthing and leaving phases, reflecting the differences in manoeuvring methods and actuator configurations. The general state-space representation is given by

$$\dot{\mathbf{x}} = \mathbf{A}\mathbf{x} + \mathbf{B}\mathbf{u} \quad (8)$$

where \mathbf{x} is the state vector; \mathbf{u} is the control input vector; \mathbf{A} is the system matrix; and \mathbf{B} is the input matrix. The specific models used for control in the unberthing (lateral and forward motions) and leaving phases are defined by Equations (9)–(11), respectively:

$$\begin{aligned} \mathbf{x} &= [\tilde{u} \quad v \quad r \quad X_d \quad Y_d \quad \psi_d]^\top \\ \mathbf{u} &= [\theta_p \quad \theta_B \quad \theta_S]^\top \\ \mathbf{A} &= \begin{bmatrix} a_{uu} & 0 & 0 & 0 & 0 & 0 \\ 0 & a_{vv} & a_{vr} & 0 & 0 & 0 \\ 0 & a_{rv} & a_{rr} & 0 & 0 & 0 \\ 1 & 0 & 0 & 0 & 0 & 0 \\ 0 & 1 & 0 & 0 & 0 & 0 \\ 0 & 0 & 1 & 0 & 0 & 0 \end{bmatrix}, \quad \mathbf{B} = \begin{bmatrix} b_{uP} & 0 & 0 \\ 0 & b_{vB} & b_{vS} \\ 0 & b_{rB} & b_{rS} \\ 0 & 0 & 0 \\ 0 & 0 & 0 \\ 0 & 0 & 0 \end{bmatrix} \end{aligned} \quad (9)$$

$$\begin{aligned} \mathbf{x} &= [\tilde{u} \quad v \quad r \quad Y_d \quad \psi_d]^\top \\ \mathbf{u} &= [\theta_p \quad \theta_B \quad \theta_S]^\top \\ \mathbf{A} &= \begin{bmatrix} a_{uu} & 0 & 0 & 0 & 0 \\ 0 & a_{vv} & a_{vr} & 0 & 0 \\ 0 & a_{rv} & a_{rr} & 0 & 0 \\ 0 & 1 & 0 & 0 & 0 \\ 0 & 0 & 1 & 0 & 0 \end{bmatrix}, \quad \mathbf{B} = \begin{bmatrix} b_{uP} & 0 & 0 \\ 0 & b_{vB} & b_{vS} \\ 0 & b_{rB} & b_{rS} \\ 0 & 0 & 0 \\ 0 & 0 & 0 \end{bmatrix} \end{aligned} \quad (10)$$

$$\begin{aligned} \mathbf{x} &= [\tilde{u} \quad v \quad r \quad Y_d \quad \psi_d]^\top \\ \mathbf{u} &= [\theta_p \quad \delta]^\top \\ \mathbf{A} &= \begin{bmatrix} a_{uu} & 0 & 0 & 0 & 0 \\ 0 & a_{vv} & a_{vr} & 0 & 0 \\ 0 & a_{rv} & a_{rr} & 0 & 0 \\ 0 & 1 & 0 & 0 & U_l \\ 0 & 0 & 1 & 0 & 0 \end{bmatrix}, \quad \mathbf{B} = \begin{bmatrix} b_{uP} & 0 \\ 0 & b_{v\delta} \\ 0 & 0 \\ 0 & 0 \\ 0 & 0 \end{bmatrix} \end{aligned} \quad (11)$$

These continuous-time models were discretized using Equation (3) and then used for the controller design. In Equations (9)–(11), the parameter values for the surge motion were taken from a linearized model previously reported in [14], whereas the parameters for the sway and yaw motions were obtained from the online model estimation.

Because the control model in this study is updated online, it constitutes a time-varying system. However, because changes in the ship speed occur gradually, the model can be regarded as time-invariant over short intervals. Therefore, a design approach for discrete-time, time-invariant systems based on the LQR algorithm was adopted. The control input is computed using the following state-feedback law:

$$\mathbf{u}(n) = -\mathbf{F}(n)\mathbf{x}(n) \quad (12)$$

where \mathbf{F} is the feedback gain matrix that minimizes the following cost function:

$$J = \sum_{t=n}^{\infty} \{ \mathbf{x}(t)^T \mathbf{Q} \mathbf{x}(t) + \mathbf{u}(t)^T \mathbf{R} \mathbf{u}(t) \} \quad (13)$$

The gain matrix \mathbf{F} is calculated based on the solution \mathbf{P} of the discrete-time algebraic Riccati equation:

$$\mathbf{P} = \mathbf{Q} + \Phi^T \mathbf{P} \Phi - \Phi^T \mathbf{P} \Gamma (\mathbf{R} + \Gamma^T \mathbf{P} \Gamma)^{-1} \Gamma^T \mathbf{P} \Phi \quad (14)$$

$$\mathbf{F} = (\mathbf{R} + \Gamma^T \mathbf{P} \Gamma)^{-1} \Gamma^T \mathbf{P} \Phi \quad (15)$$

where \mathbf{Q} and \mathbf{R} are the weighting matrices for the state and control inputs, respectively.

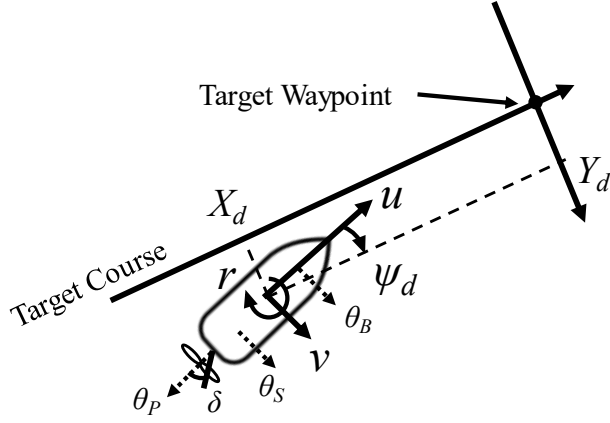


Figure 4. Coordinate system of the control system

3.4 Disturbance compensation

In the online estimation model described in Section 3.2, a bias term was introduced during the leaving phase to estimate the influence of the external force in real time. In this study, disturbance compensation was performed by computing a rudder angle correction based on the estimated bias term c_v . The rudder correction amount, denoted as $\Delta\delta$, was calculated using the following equation:

$$\Delta\delta = F_{\delta\psi} K c_v \quad (16)$$

where $F_{\delta\psi}$ is an element of the feedback gain matrix \mathbf{F} obtained in Equation (15) and K is the scaling coefficient, which was set to 16 in this study. The corrected rudder angle was then obtained by adding $\Delta\delta$ to the rudder command computed by the state feedback control law in Equation (12), and the adjusted value is used as the final control input.

3.5 Output limiting

In actual ship control, excessive actuator commands can cause an overload and lead to equipment failure. This is particularly critical for propulsion systems with propellers, such as the main propeller, B/T, and S/T, in which smooth operation is essential. To address this issue, output limiting was implemented in the control system to comply with the operational constraints of the actuators of the actual ship. For the propeller and rudder, both the upper bounds and rate-of-change limits were imposed, as shown in Table 1. For the B/T blade angle, the maximum allowable value was set to

11°, with a rate limit of 2°/s. For the S/T blade angle, the maximum value was set to 9°, with a rate limit of 2°/s. Additionally, to prevent excessive control inputs caused by sudden changes in reference values, a rate limit of 0.05 kn/s was applied to the target speed.

Table 1. Output limit value

Speed [kn] (km/h)	Propeller		Rudder
	Range [°]	Rate [°/s]	Range [°]
< 4.0 (< 7.4)	-4.0-6.0		± 35
4.0-5.0 (7.4-9.3)			± 30
5.0-6.0 (9.3-11.1)		0.25	± 25
6.0-7.0 (13.0-14.8)	1.2-8.7		± 20
7.0-8.0 (13.0-14.8)			± 15
8.0 < (14.8 <)			± 10

4 TARGET SHIP AND EXPERIMENT SCENARIO

4.1 Target ship

Sea trials were conducted using a full-scale ship to evaluate the actual sea performance of the unberthing control system based on an online estimation model. The target ship was the Shioji Maru, a training ship operated by the Tokyo University of Marine Science and Technology, as shown in Figure 5. The principal specifications of the ship are listed in Table 2. Shioji Maru is a single-shaft ship equipped with a B/T and two S/Ts. The rudder is a conventional rudder, and the main propellers, B/T and S/T, are controllable pitch propellers. During the experiments, various sensors were used for motion measurements. A GNSS navigation unit (Japan Radio Co., Ltd.) was used for the position data, a gyrocompass (YDK Technologies Co., Ltd.) for the heading and yaw rates, and a fiber-optic compass (iXblue) for the surge and sway speeds. To reduce the effect of noise on the measured data, a low-pass filter was applied to the observed sway speeds and yaw rates. In addition, to evaluate the effects of environmental disturbances, wind direction and speed were measured using an automatic weather observation system (ANEOS Corporation), and current direction and velocity were measured using an ultrasonic multilayer current profiler (Teledyne RD Instruments).



Figure 5. Shioji Maru

Table 2. Output limit value

Length overall	60.727 m
Length between perpendiculars	54.00 m
Breadth	11.10 m
Draft (average)	3.33 m
Gross tonnage	775 t

4.2 Experiment scenario

The unberthing manoeuvring plan used in the full-scale sea experiments was created based on actual unberthing manoeuvre data of the target ship from the Tsukishima Wharf in the Port of Tokyo, Japan. The planned manoeuvre is shown in Figure 6. In this plan, the unberthing manoeuvre is divided into five steps according to predefined waypoints. As shown in Figure 6, Step 1 involved a 40 m lateral movement to the port using B/T and S/T. In Step 2, the ship was accelerated to 3 kn (5.6 km/h) while maintaining its heading through attitude control using both thrusters over a 300 m forward movement. Then, from Steps 3 to 5, the ship performed a course change using a rudder while further accelerating to 8 kn (14.8 km/h). In this study, Steps 1 and 2 were designated as the unberthing phase, and Steps 3–5 were designated as the leaving phase, and were used to define the experimental scenario.

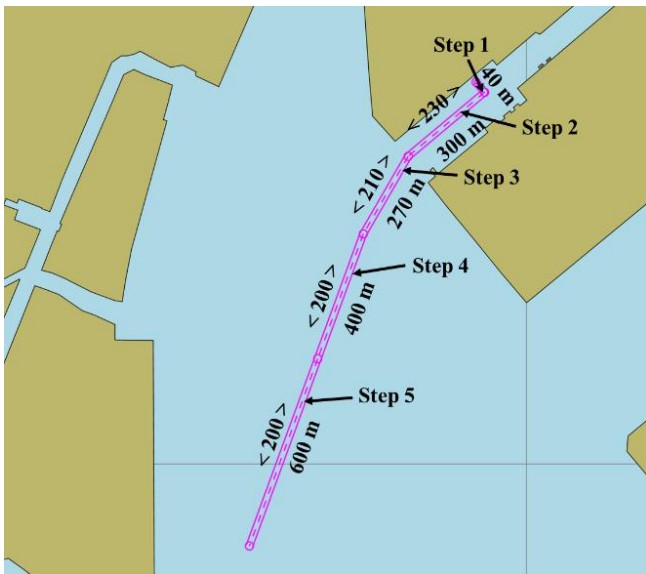


Figure 6. Manoeuvring plan

5 ACTUAL SHIP EXPERIMENT

To ensure the safety of both the vessel and nearby coastal facilities, unberthing experiments were conducted within a wide area of the bay by defining a virtual quay. The experiments were carried out using unberthing and leaving scenarios and took place off the coast of Hakkeijima in Tokyo Bay, Japan, on January 23, 2025. The initial conditions for each experiment corresponded to the starting conditions of each phase: for the unberthing phase, the ship started from the stationary state (0 kn), whereas for the leaving phase, it began moving straight ahead at 3 kn (5.6 km/h). Multiple experiments were conducted under different environmental conditions to estimate the external disturbance forces during the leaving phase. In the following sections, the experiment during the unberthing phase is referred to as Exp. 1, and those in the leaving phase are referred to as Exps. 2 and 3.

5.1 Results of unberthing phase

In this study, full-scale experimental verification was conducted using the Step 1 and Step 2 scenarios

described in Section 4 as the unberthing phase (Exp. 1). The results of Exp. 1 are shown in Figure 7. The state variables and control inputs are shown in Figure 7 (a). The left side of the figure shows, from top to bottom, the trajectory [m], surge speed u [m/s], sway speed v [m/s], and yaw rate r [°/s], while the right side shows, from top to bottom, the cross-track error (defined as X_d in Step 1 and Y_d in Step 2) [m], heading angle ψ [°], propeller blade angle θ_P [°], B/T blade angle θ_B [°], S/T blade angle θ_S [°]. Figure 7 (b) shows the wind and tidal current conditions observed during the experiment. In this figure, the wind direction indicates the direction from which the wind is blowing, and the current direction indicates the direction toward which the water is flowing. The positions and headings in Figures 7 (a) and (b) are plotted in a coordinate system, where the initial position is set to the origin and the initial heading is aligned at 0°. In the trajectory plot in Figure 7 (a), the dashed line represents the planned route, the solid line represents the actual trajectory, and the ship-shaped markers indicate the ship heading every 60 s. The horizontal axes of the other plots represent the time elapsed from the beginning of the experiment [s]. From the results, the maximum cross-track error was 1.6 m during Step 1 (lateral motion) and 7.1 m during Step 2 (forward motion). Overload warnings were not triggered for any of the actuators during the experiments. The estimated model parameters obtained from the online estimation model in Exp. 1 are shown in Figure 7 (c). The right-side graphs show, from top to bottom, φ_{vv} , φ_{rv} , γ_{vB} , and γ_{rB} , while the left-side graphs show φ_{vr} , φ_{rr} , γ_{vS} , and γ_{rS} .

The results show that throughout Exp.1, the cross-track errors remained below 10 m, which is considered acceptable from an operational standpoint, given that vessels typically move at least one ship width away from the quay during the unberthing manoeuvre. As the breadth of the target ship is 11.10 m, the observed deviation is within a tolerable range. However, in Step 2, the ship deviated from the planned route to the starboard. At approximately 520 s, both thrusters were temporarily operated in the direction opposite to that required to reduce the deviation. This was likely due to the tidal current of approximately 0.4 kn acting from the port side, with the maximum flow observed at approximately 440 s. Hence, even though the thrusters attempted to move the ship to the port, the sway speed decreased and eventually reversed direction at approximately 480 s. This reversal caused the sign of γ_{vS} to become negative, as observed around 500 s in Figure 7 (c). Consequently, the S/T was operated in a direction opposite to that needed to reduce the cross-track error, and the B/T was followed to decrease the yaw motion. Subsequently, the increased sway speed led to the recovery of the estimated parameter values. In contrast, the parameters related to the B/T, γ_{vB} and γ_{rB} , decreased as the ship's speed increased. This reflects the known characteristic that the effectiveness of the B/T worsens at higher speeds, which indicates that the model appropriately estimates the actuator effectiveness. However, at the end of the experiment, after approximately 600 s, the sign of γ_{vB} became negative. This change is linked to the unintended thruster behavior observed near 520 s, suggesting that the model parameter at this point may not be suitable for use in controller design and requires further countermeasures.

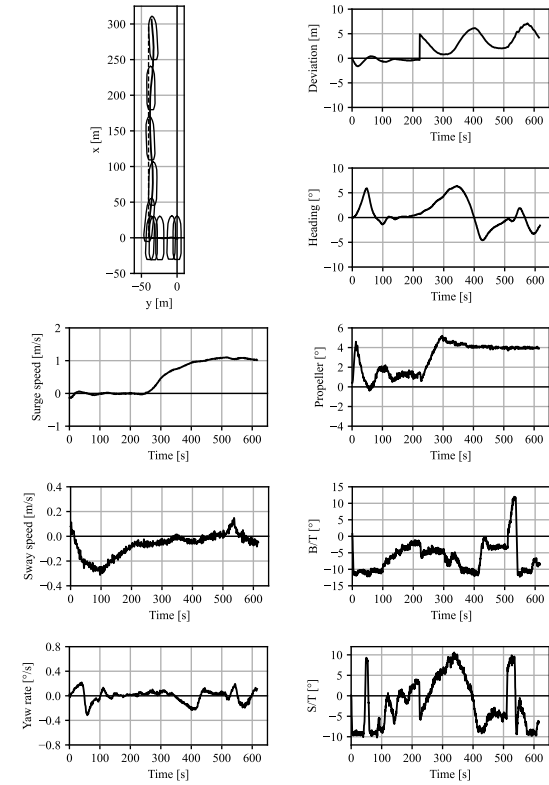
5.2 Results of leaving phase

In this study, Steps 3–5 described in Section 4 were used as the leaving phase scenarios, and a full-scale experimental verification was conducted using Exp. 2 and 3. The results are presented in Figures 8 and 9. The graph layout in Figures 8 and 9 (a) follows the same format as that in Figure 7 (a), but the actuators used are rudders instead of thrusters. Figures 8 and 9 (b) show the wind and tidal current conditions measured during the experiments, whereas Figures 8 and 9 (c) show the parameters estimated by the online model. In Figures 8 and 9 (c), the left-side graphs show, from top and bottom, ϕ_{vv} , ϕ_{rv} , $\gamma_{v\delta}$, and c_v , while the left-side graphs show, ϕ_{vr} , ϕ_{rr} , and $\gamma_{r\delta}$ from top to bottom. Table 3 summarizes the maximum cross-track errors observed at each step.

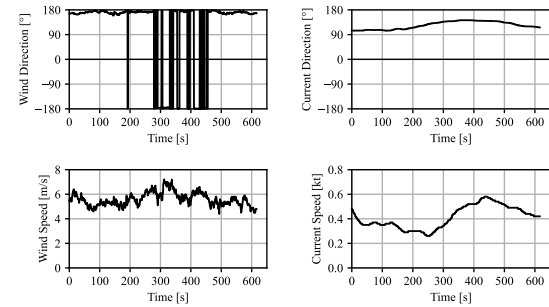
Based on Figures 8 and 9 (a) and Table 3, both Exp. 2 and 3 showed successful route-tracking when the ship was accelerating. The cross-track errors remained within 5 m throughout Steps 3–5, indicating accurate control performance during the leaving phase. Furthermore, from Figures 8 and 9 (c), the rudder-related parameters $\gamma_{v\delta}$ and $\gamma_{v\delta}$ increased as the ship accelerated, which reflects increasing rudder effectiveness at higher speeds. This suggests that the model estimation appropriately captured the rudder dynamics. However, the bias term c_v in the model estimation was estimated in the port-side (negative) direction, starting at approximately 200 s after the heading change in both experiments. Although direct observation of the external forces acting on a ship under actual sea conditions is not possible, the measured wind and current conditions as well as the observed sway speeds indicate that the ship likely experienced a port-side disturbance. Looking at the cross-track errors in Figures 8 and 9, the ship moved to starboard in both experiments, which was opposite to the direction of the sway speed. This behavior suggests that the disturbance compensation based on the bias term c_v is effective in counteracting external forces.

Table 3. Maximum deviation of each step

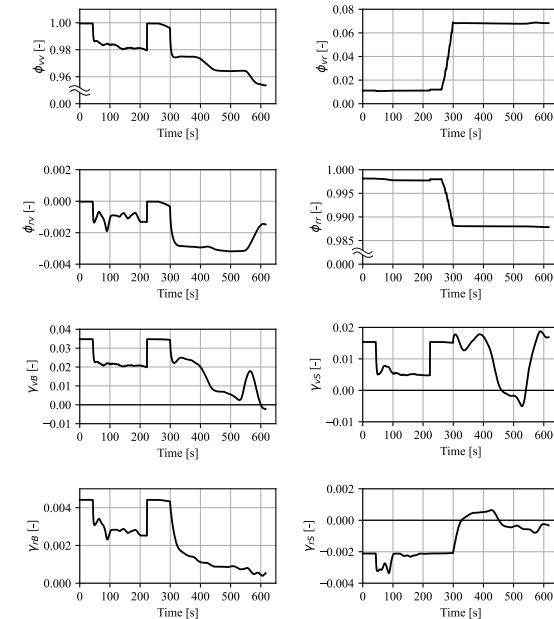
	Step 3	Step 4	Step 5
Exp. 2	1.4 m	-4.1 m	-3.5 m
Exp. 3	3.1 m	-4.0 m	-3.9 m



(a) Ship state and control inputs

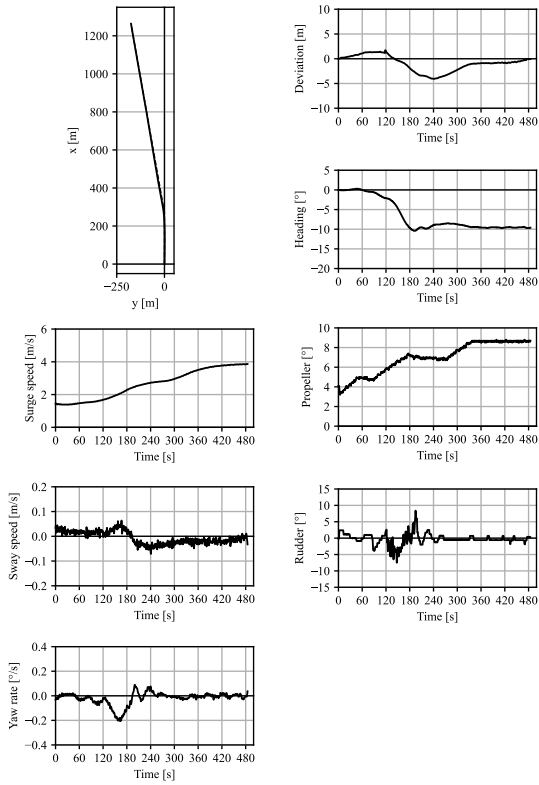


(b) Disturbance conditions

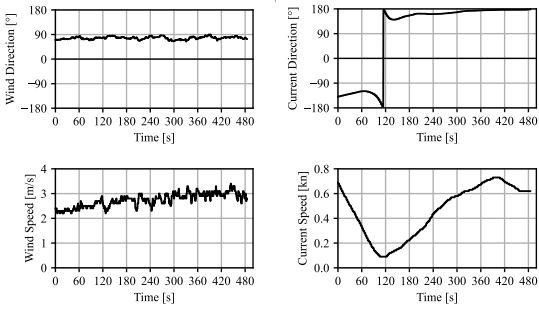


Estimated parameters

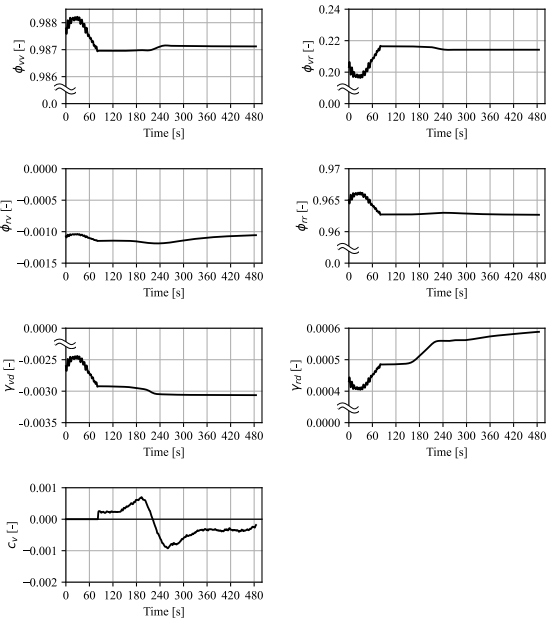
Figure 7. Results of Exp.1



(a) Ship state and control inputs

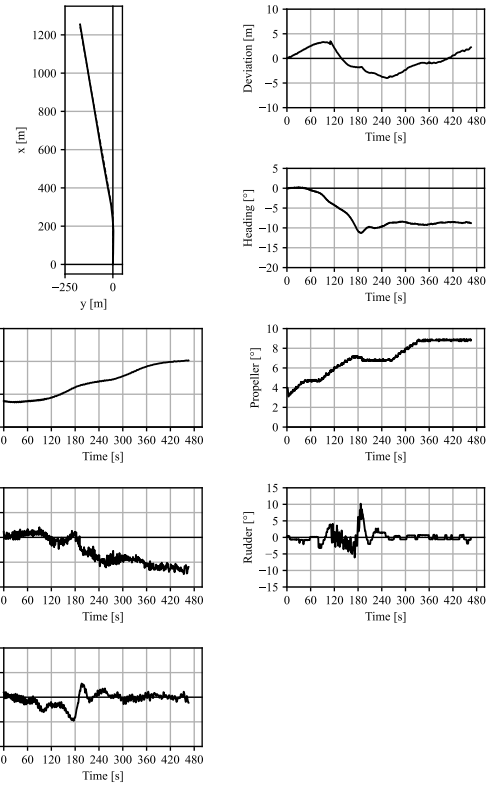


(b) Disturbance conditions

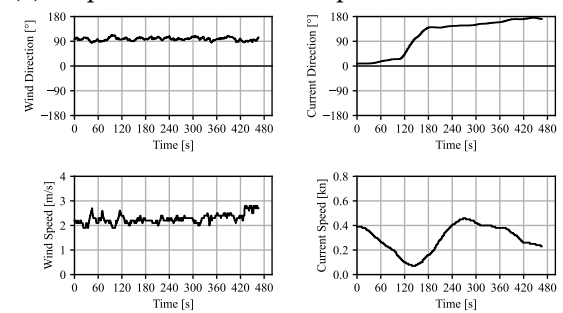


(c) Estimated parameters

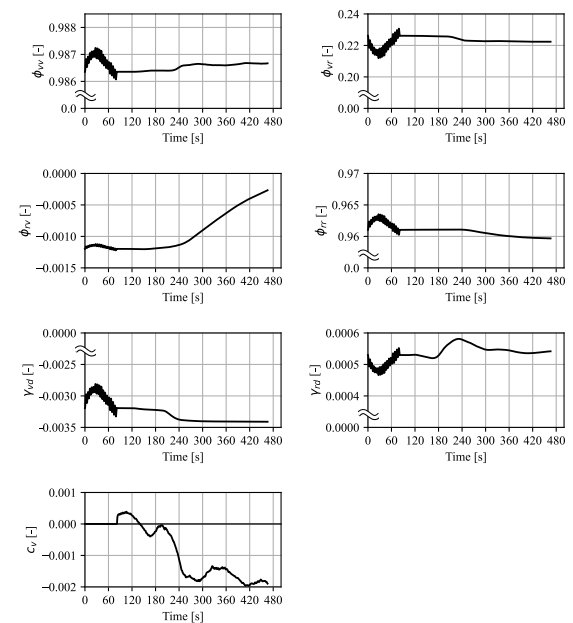
Figure 8. Results of Exp. 2



(a) Ship state and control inputs



(b) Disturbance conditions



(c) Estimated parameters

Figure 9. Results of Exp. 3

6 CONCLUSION

In this study, sea experiments were conducted using a full-scale vessel to evaluate the actual sea performance of an unberthing control system based on an online estimation model that updates the motion model parameters from the time-series data of ship velocity and control inputs. The experimental scenarios were designed based on actual unberthing operations and were divided into two phases: unberthing and leaving. To ensure safety, experiments were conducted over a wide area of the bay using a virtual quay setup. The experimental results demonstrate that the proposed system achieves accurate route tracking in both the unberthing and leaving phases. Furthermore, in the leaving phase, the disturbance compensation based on the estimated bias term successfully identified the direction of the disturbance and generated control inputs to compensate for its effect. The results indicate that the proposed control system can accurately perform unberthing manoeuvres under actual sea conditions. However, during the unberthing phase, unstable control behaviour was observed in the segments where the accuracy of the model estimation deteriorated. This suggests the need for further improvement which could involve the development of reliability assessment methods that can prevent low-accuracy model estimates from being used in the controller design.

ACKNOWLEDGEMENT

The authors express their gratitude to the crew of Shioji Maru for their cooperation in conducting the ship experiments in this study. This study was supported by JST SPRING under Grant JPMJSP2147.

REFERENCES

- [1] International Maritime Organization, "Results of demonstration tests of fully autonomous ship navigation on 'MEGURI 2040'", submitted by Japan, IMO MSC 106/INF. 4, 2022.
- [2] H. Yasukawa and Y. Yoshimura, "Introduction of MMG standard method for ship manoeuvring predictions", *Journal of Marine Science and Technology*, Vol. 20, pp. 37–52, 2015.
- [3] L. P. Perera, P. Oliveira, and C. G. Soares, "System identification of nonlinear vessel steering", *Journal of Offshore Mechanics and Arctic Engineering*, Vol. 137, 031302, 2015.
- [4] Y. Miyachi, A. Maki, N. Umeda, D. M. Rachman, and Y. Akimoto, "System parameter exploration of ship manoeuvring model for automatic docking/berthing using CMA-ES", *Journal of Marine Science and Technology*, Vol. 27, pp. 1065–1083, 2022.
- [5] X. -G. Zhang and Z. -J. Zou, "Identification of Abkowitz model for ship manoeuvring motion using ε -support vector regression", *Journal of Hydrodynamics*, Vol. 23, pp. 353–360, 2011.
- [6] Y. Yoshimura, "Mathematical model for manoeuvring ship motion (MMG model)", *Workshop on Mathematical Models for Operations involving Ship-Ship Interaction*, pp. 1–6, 2005.
- [7] K. Kijima, T. Katsuno, Y. Nakiri, and Y. Furukawa, "On the manoeuvring performance of a ship with the parameter of loading condition", *Journal of the Society of Naval Architects of Japan*, Vol. 168, pp. 141–148, 1990.
- [8] K. Hasegawa, "On a performance criterion of autopilot navigation", *Journal of the Kansai Society of Naval Architects, Japan*, Vol. 178, pp. 93–103, 1980.
- [9] T. Okazaki and K. Ohtsu, "A study on mathematical manoeuvring model to solve minimum time approaching problems", *The Journal of Japan Institute of Navigation*, Vol. 114, pp. 141–149, 2006.
- [10] S. Miyoshi, Y. Hara, and K. Ohtsu, "Study on optimum tracking control with linearized model for vessel", *The Journal of Japan Institute of Navigation*, Vol. 117, pp. 183–189, 2007.
- [11] S. Miyoshi, T. Ioki, and I. Suzuki, "Development of autonomous manoeuvring system for realizing fully autonomous ships -preliminary report on actual sea test and tracking control", *Conference Proceedings The Japan Society of Naval Architects and Ocean Engineers*, Vol. 34, pp. 195–201, 2022.
- [12] T. Ioki and S. Miyoshi, "Development of manoeuvring system for realizing autonomous ships – on approach manoeuvring control using model-based prediction", *Conference Proceedings The Japan Society of Naval Architects and Ocean Engineers*, Vol. 34, pp. 51–56, 2022.
- [13] Y. Meng, X. Zhang, X. Zhang, D. Ma, and Y. Duan, "Online ship motion identification modeling and its application to course-keeping control", *Ocean Engineering*, Vol. 294, 116853, 2024.
- [14] H. Kashiwagi and T. Okazaki, "Ship control of unberthing manoeuvring using an online estimation model under disturbance", *SICE Journal of Control, Measurement, and System Identification*, Vol. 18, Issue 1, 2474299, 2025.
- [15] H. Kashiwagi and T. Okazaki, "Ship control of unberthing manoeuvring using a sequential estimation model", *2024 SICE Festival with Annual Conference (SICE FES)*, pp. 672–677, 2024.